

# Efficient PHY Layer Abstraction under Imperfect Channel Estimation

Liu Cao, Lyutianyang Zhang, Sian Jin, and Sumit Roy, *Fellow, IEEE*

**Abstract**—As most existing work investigate the PHY layer abstraction under an assumption of perfect channel estimation, it may become unreliable if there exists channel estimation error in a real communication system. This letter improves an efficient PHY layer method, EESM-log-SGN PHY layer abstraction, by considering the presence of channel estimation error. We develop two methods for implementing the EESM-log-SGN PHY abstraction under imperfect channel estimation. We show that the effective SINR is not impacted by the channel estimation error under multiple-input and single-output (MISO)/single-input and single-output (SISO) configuration, which is also verified by the full PHY simulation. The developed methods are then validated under different orthogonal frequency division multiplexing (OFDM) scenarios.

**Index Terms**—PHY layer abstraction, EESM-log-SGN, L2S, MMSE receiver.

## I. INTRODUCTION

FULL PHY (link) simulations, which typically run on link simulators, quantify the network performance in Wi-Fi (IEEE 802.11 WLANs) systems from the packet-level performance metrics. However, running a full PHY simulation that involves generating channel realizations and transceiver signal processing is impractical within a network simulator [1]. In addition, with increasing node density and complexity in the PHY layer, associated computational complexity is also a major concern for network simulators [2]. To cope with such issues, *PHY layer abstraction*<sup>1</sup> is used to generate accurate link performance in a network simulator. In particular, a novel EESM-log-SGN PHY layer abstraction method<sup>2</sup> achieves good accuracy in modeling the PHY layer performance, meanwhile, its runtime is insensitive to system dimensionality change and is much reduced as compared to the traditional PHY layer abstraction methods.

To achieve PHY layer abstraction of current Wi-Fi systems which operate over wideband frequency-selective fading channels, link-to-system (L2S) mapping has been widely adopted [3]–[8]. L2S mapping function translates the post processing

Signal-to-Interference-plus-Noise-Ratio (SINR) matrix into a single scalar metric called the *effective SINR* [9]. Abstracting the post processing SINRs over all subcarriers and spatial streams using a single valued effective SINR significantly simplifies the L2S interface [8], [10]. The effective SINR is a convenient metric to describe the packet-level performance in a network simulator, at the cost of losing detail for each spatial stream (symbol-level performance), and fully align with the packet-level performance obtained from the full PHY simulations.

In any communication system, channel estimation is implemented by the receiver. However, the estimated channel is inherently noisy in practical systems, which incurs channel estimation error. Such channel estimation error may severely impact the post processing SINR, further impacting the effective SINR which characterizes the results related to PHY layer abstraction. To the best knowledge of the author of this letter, the channel estimation error was hardly investigated in PHY layer abstraction as the channel estimation was assumed to be noise free in previous work. As a result, one key issue arises that the PHY layer abstraction executed under perfect channel estimation may become no longer reliable since any real communication system cannot perform perfect channel estimation.

Motivated by the aforementioned issues, it is necessary to investigate the PHY layer abstraction impacted by the channel estimation error. This letter develops the EESM-log-SGN PHY layer abstraction in the presence of the channel estimation error, which accords with the current PHY layer abstraction implementation as well as the MIMO architecture of typical Wi-Fi systems. Meanwhile, an analytical model is proposed to capture the relation between the channel estimation error and the effective SINR. The analytical effective SINRs are further utilized to develop the EESM-log-SGN PHY layer abstraction.

## II. SYSTEM ARCHITECTURE

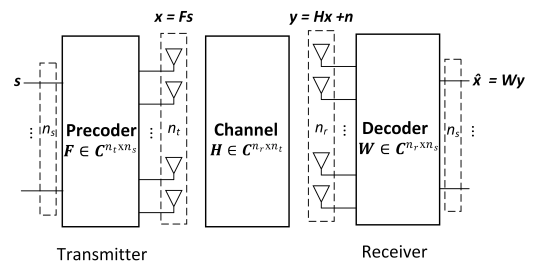


Fig. 1: MIMO architecture of typical Wi-Fi systems.

Liu Cao, Lyutianyang Zhang, and Sumit Roy are with the Department of Electrical and Computer Engineering, University of Washington, Seattle, WA 98195 USA (e-mail: liucuo@uw.edu; lyutiz@uw.edu; sroy@uw.edu). Sian Jin is with the Department of Electrical and Computer Engineering, Princeton University, Princeton, NJ 08544 USA (sj2434@princeton.edu) (*Corresponding author: Liu Cao.*)

<sup>1</sup>The PHY layer abstraction in a network simulator is the packet error model that produces a decision on whether the packet is successfully received or not based on the PHY layer setup.

<sup>2</sup>EESM-log-SGN PHY layer abstraction [1] bypasses the matrix calculation steps required by the traditional PHY layer abstraction methods, and directly models effective SINR by using a 4-parameter distribution called log-SGN distribution.

### A. MIMO Architecture

The multiple-input and multiple-output (MIMO) architecture of typical Wi-Fi systems is depicted in Fig. 1. The transmitted signal and the received signal can be described with the following equation

$$\hat{\mathbf{x}} = \mathbf{W}\mathbf{H}\mathbf{F}\mathbf{s} + \mathbf{W}\mathbf{n}, \quad (1)$$

where  $\mathbf{x} \in \mathbb{C}^{n_r}$ ,  $\mathbf{W} \in \mathbb{C}^{n_s \times n_r}$ ,  $\mathbf{H} \in \mathbb{C}^{n_r \times n_t}$ ,  $\mathbf{F} \in \mathbb{C}^{n_t \times n_s}$ ,  $\mathbf{s} \in \mathbb{C}^{n_s}$ , and  $\mathbf{n} \in \mathbb{C}^{n_r}$  denote the baseband signal at the receiver, decoding matrix, channel matrix, precoding matrix, baseband signal at the transmitter, and the noise vector at the receiving antenna which conforms to zero mean circularly symmetric complex Gaussian (ZMCSG) with variance  $\sigma^2$ . In our work, we employ the minimum mean squared error (MMSE) detector which is expressed as [11], [12]

$$\mathbf{W} = \left[ (\mathbf{H}\mathbf{F})^* \mathbf{H}\mathbf{F} + \frac{\mathbf{I}}{\text{SNR}} \right]^{-1} (\mathbf{H}\mathbf{F})^*, \quad (2)$$

where  $\text{SNR} = \frac{\mathbb{E}[(\mathbf{F}\mathbf{s})^* (\mathbf{F}\mathbf{s})]}{\mathbb{E}[\mathbf{n}^* \mathbf{n}]}$  represents the ratio between the signal energy at each transmit antenna and the noise energy, and  $\mathbf{I}$  represents the identity matrix.

As is shown in Fig. 2, a desired transmitter transmits  $n_s$  spatial streams (independent information flows) to a single user using the set of subcarriers  $\mathcal{N}_{sc}$  through Orthogonal Frequency Division Multiplexing (OFDM) in a single basic service set (BSS). On each subcarrier  $i \in \mathcal{N}_{sc}$ , the modulated  $n_s$  spatial streams are then mapped into  $n_t$  transmit antennas using a  $n_t \times n_s$  precoding matrix  $\mathbf{F}_i$  for subcarrier  $i$  [9]. The desired transmitted packet is passed through the  $n_r \times n_t$  frequency-domain channel matrices  $\mathbf{H}_i, i \in \mathcal{N}_{sc}$  and arrives at the  $n_r$  receive antennas of receiver. The frequency-domain channel matrices  $\mathbf{H}_i$  characterizes the frequency-selectivity property in which  $\mathbf{H}_i$  varies with subcarrier index  $i$  under a frequency-selective channel.

### B. Link-to-system (L2S) mapping

At receiver's  $i$ -th subcarrier  $i \in \mathcal{N}_{sc}$  and for stream  $j \in \{1, 2, \dots, n_s\}$ , the post processing SINR  $\Gamma_{i,j}$  is [4]

$$\Gamma_{i,j} = \frac{S_{i,j}}{I_{i,j}^s + N_{i,j}}, \quad (3)$$

where  $S_{i,j}$  is the received signal power,  $I_{i,j}^s$  is the inter-stream interference, and  $N_{i,j}$  is the post processing noise power. By [4], we have  $S_{i,j} = P_t |[\mathbf{W}_i]_j^* \mathbf{H}_i [\mathbf{F}_i]_j|^2$ ,  $I_{i,j}^s = P_t \|\mathbf{W}_i\|_j^* \mathbf{H}_i \mathbf{F}_i\|^2 - S_{i,j}$ , and  $N_{i,j} = \sigma^2 \|\mathbf{W}_i\|_j\|^2$ , where  $P_t$  is the received signal power at receiver from the desired transmitter,  $\sigma^2$  is additive noise power on each subcarrier of receiver,  $[\cdot]_j$  denotes the  $j$ -th column of a matrix, and  $\|\cdot\|$  is the Euclidean norm of a vector. The post processing SINR matrix at receiver is defined by  $\mathbf{\Gamma} \triangleq (\Gamma_{i,j})_{i \in \mathcal{N}_{sc}, 1 \leq j \leq n_s}$ , which reflects channel frequency-selectivity, antenna correlation captured by  $\mathbf{H}_i, i \in \mathcal{N}_{sc}$ , and transmit beamforming gain captured by  $\mathbf{F}_i, i \in \mathcal{N}_{sc}$  [1].

An L2S mapping function  $\Phi$  then compresses the post processing SINRs on different subcarriers and streams into an effective SINR, which would yield the same instantaneous PER if the simulation was run for an AWGN-SISO channel. The effective SINR at receiver is [3]–[6]

$$\Gamma_{eff}^{sirr} = \alpha \Phi^{-1} \left( \frac{1}{n_{sc} n_s} \sum_{i \in \mathcal{N}_{sc}} \sum_{j=1}^{n_s} \Phi \left( \frac{\Gamma_{i,j}}{\beta} \right) \right), \quad (4)$$

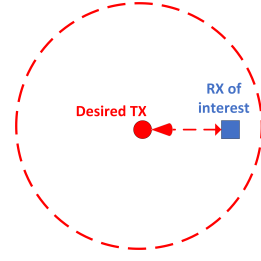


Fig. 2: Single BSS single user OFDM scenario.

where  $\Phi^{-1}$  is the inverse L2S mapping function,  $\mathcal{N}_{sc}$  is the set of subcarriers,  $n_{sc} \triangleq |\mathcal{N}_{sc}|$  is the number of subcarriers allocated to the receiver,  $n_s$  is the number of spatial streams sent to the receiver,  $\alpha$  and  $\beta$  are L2S mapping tuning parameters that depend on PHY layer configurations (channel type, OFDM MIMO setup, MCS and channel coding). The accuracy of the instantaneous PER prediction depends on the L2S mapping function  $\Phi$ , such as Exponential Effective SINR Mapping (EESM) and Received Bit Information Rate (RBIR) mapping. In particular, EESM L2S mapping function is used in our work. For EESM L2S mapping,  $\alpha = \beta$  and L2S mapping function  $\Phi(x) = \exp(-x)$  [6]. Then, Eq. (4) reduces to [4]

$$\Gamma_{eff}^{sirr} = -\beta \ln \left( \frac{1}{n_{sc} n_s} \sum_{i \in \mathcal{N}_{sc}} \sum_{j=1}^{n_s} \exp \left( -\frac{\Gamma_{i,j}}{\beta} \right) \right). \quad (5)$$

## III. SYSTEM MODEL

### A. Simulation based PHY layer abstraction

The definition of the post processing SINR  $\Gamma_{i,j}$  expressed in Eq. (3) holds if the channel is perfectly known at the receiver. However, in any real system, the channel matrix at any subcarrier  $\mathbf{H}_i, \forall i \in \mathcal{N}_{sc}$  estimated by the receiver is inherently noisy, so we model the channel matrix as

$$\hat{\mathbf{H}}_i = \mathbf{H}_i + \Delta \mathbf{H}_i, \quad (6)$$

where  $\Delta \mathbf{H}_i$  denotes the estimation error matrix assumed to be uncorrelated with  $\mathbf{H}_i$ , and each entry of  $\mathbf{H}_i$  follows ZMCSG with variance  $\sigma_e^2$  [3]. The quality of channel estimation is captured by  $\sigma_e^2$ , which can be appropriately estimated depending on the channel estimation method. We assume that each block (packet), that undergoes a different channel realization  $\mathbf{H}_i$ , observes a different realization of  $\Delta \mathbf{H}_i$  at the receiver. As a result, the packet-level performance may be significantly impacted by the quality of the channel estimation.

As is shown in Fig. 3, we first demonstrate the simulation-based flow chart that consists of the simulation steps and statistical steps. In the simulation steps, we develop the full PHY simulation [4] considering imperfect channel estimation. Based on the developed the full PHY simulation, we can obtain the packet-level performance under imperfect channel estimation. Fig. 4 shows the average PER regarding the SNR under perfect and imperfect channel estimation through the full

<sup>3</sup>The channel estimation noise variance can be defined as  $\sigma_e^2 = \frac{1}{n_t \text{SNR}}$  [13].

<sup>4</sup>The full PHY simulation is conducted using a credible link simulator (e.g., MATLAB WLAN Toolbox) to provide calibrated L2S mapping tuning parameters.

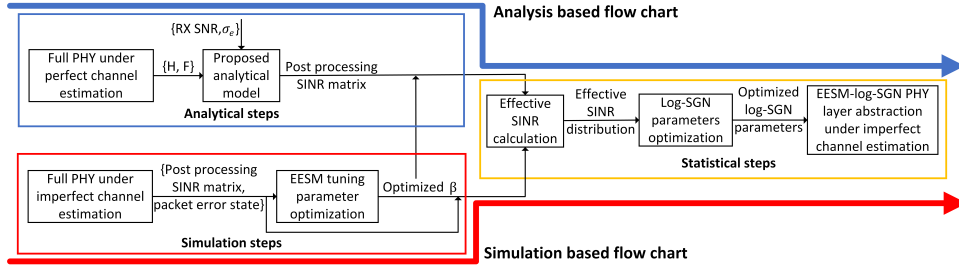


Fig. 3: Flow charts for implementing EESM-log-SGN PHY layer abstraction under imperfect channel estimation.

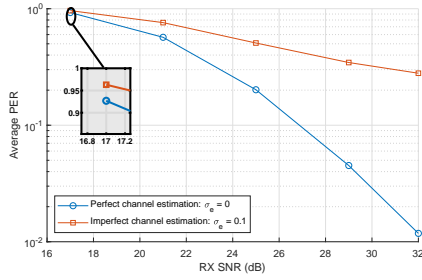


Fig. 4: Full PHY simulation: Average PER versus SNR under OFDM allocation with 242 subcarriers,  $2 \times 2$  MIMO, IEEE TGax channel model-B, MCS5.

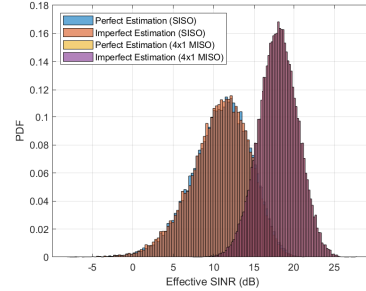


Fig. 5: Effective SINR distributions following simulation steps (SNR = 13dB).

PHY simulation. One can observe that a small  $\sigma_e$  can cause large PER difference between different channel estimation qualities in each SNR points.

Subsequently, the post processing SINR matrix and the associated binary packet error state<sup>5</sup> for each packet can be obtained after the full PHY simulation. The set {post processing SINR matrix  $\Gamma$ , binary packet error state} are then used to optimize the EESM tuning parameter  $\beta$  of the EESM mapping function [17]. The parameter  $\beta$  in Eq. (4) is then optimized to minimize the mean square error (MSE) between the instantaneous PER-effective SINR curve for the simulated frequency-selective fading channel and the instantaneous PER-SNR curve under the AWGN-SISO channel. Then, in the initial stage of the statistical steps, an effective SINR distribution can be obtained through Eq. (4) with the optimized EESM parameter  $\beta$  and post processing SINR matrices of all packets.

**Lemma 1.** *The effective SINR  $\Gamma_{eff}^{sinr}$  is irrelevant to the channel estimation error  $\sigma_e$  under MISO/SISO configuration.*

*Proof.* Under MISO configuration,  $\mathbf{W}_i$  becomes a scalar, i.e.,  $W_i$ , as  $n_r = 1$  and  $n_s = 1$ . For the  $i$ -th subcarrier  $i \in \mathcal{N}_{sc}$  and the only stream (indicating  $I_{i,1}^s = 0$ ), the post processing SINR  $\Gamma_{i,1}$  is expressed as  $\Gamma_{i,1} = \frac{S_{i,1}}{N_{i,1}}$ , where  $S_{i,1} = P_t |[W_i]_1^* \mathbf{H}_i [\mathbf{F}_i]_1|^2 = P_t W_i^2 |\mathbf{H}_i [\mathbf{F}_i]_1|^2$ , and  $N_{i,1} = \sigma^2 |[W_i]_1|^2 = \sigma^2 W_i^2$ . Substitute  $S_{i,1}$  and  $N_{i,1}$  with the above extended terms, we get  $\Gamma_{i,1} = \frac{P_t |\mathbf{H}_i [\mathbf{F}_i]_1|^2}{\sigma^2}$ . Similarly, under SISO configuration,  $\mathbf{W}_i$ ,  $\mathbf{H}_i$  and  $\mathbf{F}_i$  are all

scalars, i.e.,  $W_i$ ,  $H_i$  and  $F_i$ , as  $n_r = 1$ ,  $n_s = 1$  and  $n_t = 1$ . Hence  $S_{i,1} = P_t |[W_i]_1^* H_i F_i|^2 = P_t W_i^2 H_i^2 F_i^2$  and  $N_{i,1} = \sigma^2 |[W_i]_1|^2 = \sigma^2 W_i^2$ . Then we get  $\Gamma_{i,1} = \frac{P_t H_i^2 F_i^2}{\sigma^2}$ . Hence based on Eq. (5), the effective SINR under both configurations becomes  $\Gamma_{eff}^{sinr} = -\beta \Phi^{-1} \left( \frac{1}{n_{sc}} \sum_{i \in \mathcal{N}_{sc}} \Phi \left( \frac{\Gamma_{i,1}}{\beta} \right) \right)$ , which is irrelevant to  $W_i$  impacted by  $\sigma_e$ . ■

**Remark 1.** *According to Lemma 1, the channel estimation error does not impact effective SINR distribution under MISO/SISO configuration. However, this does not hold under MIMO/SIMO configuration as the MMSE equalizer,  $\mathbf{W}_i$ , cannot be cancelled when calculating the post processing SINR.*

As Fig.5 shows, the effective SNR distributions following the simulation steps overlap in the MISO/SISO case under the perfect and imperfect channel estimation. In the statistical steps, the obtained effective SINR distribution is then statistically fitted with the log-SGN distribution [1] which is defined as

$$X \triangleq \ln(\Gamma_{eff}^{sinr}) \sim \text{SGN}(\hat{\mu}, \hat{\sigma}, \hat{\lambda}_1, \hat{\lambda}_2), \quad (7)$$

with PDF

$$f_X(x; \hat{\mu}, \hat{\sigma}, \hat{\lambda}_1, \hat{\lambda}_2) = \frac{2}{\hat{\sigma}} \psi \left( \frac{x - \hat{\mu}}{\hat{\sigma}} \right) \Psi \left( \frac{\hat{\lambda}_1 (x - \hat{\mu})}{\sqrt{\hat{\sigma}^2 + \hat{\lambda}_2 (x - \hat{\mu})^2}} \right), \quad x \in \mathbf{R}, \quad (8)$$

where  $\hat{\mu} \in \mathbf{R}$  is the location parameter,  $\hat{\sigma} > 0$  is the scale parameter,  $\hat{\lambda}_1 \in \mathbf{R}$  and  $\hat{\lambda}_2 \geq 0$  are shape parameters,  $\psi(x)$  is the standard normal PDF, and  $\Psi(x)$  is the standard normal cumulative distribution function. As the effective SINRs for log-SGN fitting are based on full PHY simulation results under imperfect channel estimation, the four log-SGN parameters

<sup>5</sup>The frequency-selective channel instance is assumed to be almost invariant during the transmission of each packet (e.g., IEEE TGax channel models [14]) and different channel instances for different packets are assumed to be i.i.d. [5], [15], [16].

$$\mathbf{E}_i = \left( \begin{array}{l} \sigma_e^2 \text{tr}(\mathbf{K}_i \mathbf{F}_i^* \mathbf{H}_i^* \mathbf{H}_i \mathbf{F}_i \mathbf{F}_i^* \mathbf{H}_i^* \mathbf{H}_i \mathbf{F}_i \mathbf{K}_i^*) \mathbf{K}_i \mathbf{F}_i^* \mathbf{H}_i^* \mathbf{H}_i \mathbf{F}_i \mathbf{K}_i^* + \sigma_e^2 \text{tr}(\mathbf{H}_i \mathbf{F}_i \mathbf{K}_i \mathbf{F}_i^* \mathbf{H}_i^* \mathbf{H}_i \mathbf{F}_i \mathbf{F}_i^* \mathbf{H}_i^* \mathbf{H}_i \mathbf{F}_i \mathbf{K}_i^* \mathbf{F}_i^* \mathbf{H}_i^*) \mathbf{K}_i \mathbf{K}_i^* \\ - \sigma_e^2 \text{tr}(\mathbf{H}_i \mathbf{F}_i \mathbf{K}_i \mathbf{F}_i^* \mathbf{H}_i^* \mathbf{H}_i \mathbf{F}_i \mathbf{F}_i^* \mathbf{H}_i^*) \mathbf{K}_i \mathbf{K}_i^* - \sigma_e^2 \text{tr}(\mathbf{H}_i \mathbf{F}_i \mathbf{F}_i^* \mathbf{H}_i^* \mathbf{H}_i \mathbf{F}_i \mathbf{K}_i^* \mathbf{F}_i^* \mathbf{H}_i^*) \mathbf{K}_i \mathbf{K}_i^* \\ + \sigma_e^2 \text{tr}(\mathbf{H}_i \mathbf{F}_i \mathbf{F}_i^* \mathbf{H}_i^*) \mathbf{K}_i \mathbf{K}_i^* + \text{SNR}^{-1} \mathbf{W}_i \mathbf{W}_i^* \end{array} \right) \quad (9)$$

$$\mathbf{N}_i = \left( \begin{array}{l} \text{SNR}^{-1} \mathbf{W}_i \mathbf{W}_i^* + \text{SNR}^{-1} \sigma_e^2 \text{tr}(\mathbf{K}_i \mathbf{F}_i^* \mathbf{H}_i^* \mathbf{H}_i \mathbf{F}_i \mathbf{K}_i^*) \mathbf{K}_i \mathbf{F}_i^* \mathbf{H}_i^* \mathbf{H}_i \mathbf{F}_i \mathbf{K}_i^* \\ + \text{SNR}^{-1} \sigma_e^2 \text{tr}(\mathbf{H}_i \mathbf{F}_i \mathbf{K}_i \mathbf{F}_i^* \mathbf{H}_i^* \mathbf{H}_i \mathbf{F}_i \mathbf{K}_i^* \mathbf{F}_i^* \mathbf{H}_i^*) \mathbf{K}_i \mathbf{K}_i^* - \text{SNR}^{-1} \sigma_e^2 \text{tr}(\mathbf{H}_i \mathbf{F}_i \mathbf{K}_i \mathbf{F}_i^* \mathbf{H}_i^*) \mathbf{K}_i \mathbf{K}_i^* \\ - \text{SNR}^{-1} \sigma_e^2 \text{tr}(\mathbf{H}_i \mathbf{F}_i \mathbf{K}_i^* \mathbf{F}_i^* \mathbf{H}_i^*) \mathbf{K}_i \mathbf{K}_i^* + \text{SNR}^{-1} \sigma_e^2 N_r \mathbf{K}_i \mathbf{K}_i^* \end{array} \right) \quad (10)$$

summarize the key information in the PHY layer in the existence of channel estimation error.

### B. Analysis based PHY layer abstraction

Fig. 3 shows an analysis based flow chart to achieve the EESM-log-SGN PHY layer abstraction under imperfect channel estimation. This flow chart includes the analytical steps as well as the statistical steps. In the analytical steps, we use the full PHY simulation under perfect channel estimation to track the (perfect) channel realization information (i.e., channel matrix  $\mathbf{H}_i$ ,  $i \in \mathcal{N}_{sc}$  and precoding matrix  $\mathbf{F}_i$ ,  $i \in \mathcal{N}_{sc}$  of each packet). Then an analytical model is developed to characterize the relation between the channel estimation error and the effective SINR. The developed analytical model relies on the SNR, channel estimation error  $\sigma_e^2$  and the information from the full PHY simulation under perfect channel estimation. After the analytical steps, the analytical post processing SINRs under imperfect channel estimation are obtained. Then we can develop the EESM-log-SGN PHY abstraction considering channel estimation error based on the analytical effective SINR distribution which is processed by the statistical steps. Note that given a fixed SNR, different packets characterize different  $\hat{\Gamma}_{eff}^{sindr}$  due to the block fading channels. Thus, the analytical steps output a distribution rather than a number. In the rest of this section, we present the analytical model of effective SINR for MMSE detector with channel estimation error.

Following Eq. (2), the receiver can use the imperfect estimated channel to calculate the MMSE detector as follows,

$$\begin{aligned} \hat{\mathbf{W}}_i &= [(\mathbf{H}_i \mathbf{F}_i + \Delta \mathbf{H}_i \mathbf{F}_i)^* (\mathbf{H}_i \mathbf{F}_i + \Delta \mathbf{H}_i \mathbf{F}_i) + \frac{\mathbf{I}}{\text{SNR}}]^{-1} \bullet \\ &\quad (\mathbf{H}_i \mathbf{F}_i + \Delta \mathbf{H}_i \mathbf{F}_i)^* \\ &= [\mathbf{F}_i^* \mathbf{H}_i^* \mathbf{H}_i \mathbf{F}_i + \frac{\mathbf{I}}{\text{SNR}} + \mathbf{F}_i^* \mathbf{H}_i^* \Delta \mathbf{H}_i \mathbf{F}_i \\ &\quad + \mathbf{F}_i^* \Delta \mathbf{H}_i^* \mathbf{H}_i \mathbf{F}_i]^{-1} \bullet \mathbf{F}_i^* (\mathbf{H}_i + \Delta \mathbf{H}_i)^*, \end{aligned} \quad (11)$$

where we ignore the term  $\mathbf{F}_i^* \Delta \mathbf{H}_i^* \Delta \mathbf{H}_i \mathbf{F}_i$  since it is much less significant than the channel estimation error  $\Delta \mathbf{H}_i$  when  $\sigma_e^2$  is small. With imperfect channel estimation,  $\Delta \mathbf{H}_i$ , the imperfect MMSE solution can also be written as  $\hat{\mathbf{W}}_i = \mathbf{W}_i + \Delta \mathbf{W}_i$ . Thus the MMSE estimate of the signal vector becomes

$$\hat{\mathbf{x}}_i = \hat{\mathbf{W}}_i \mathbf{y}_i = \mathbf{W}_i \mathbf{H}_i \mathbf{x}_i + \Delta \mathbf{W}_i \mathbf{H}_i \mathbf{x}_i + \mathbf{W}_i \mathbf{n}_i + \Delta \mathbf{W}_i \mathbf{n}_i, \quad (12)$$

where  $\mathbf{x} = \mathbf{F}\mathbf{s}$  represents the precoded base-band data streams, and  $\mathbf{s}$  is the original signal. Denote  $\mathbf{K}_i = (\mathbf{H}_i^* \mathbf{F}_i^* \mathbf{F}_i \mathbf{H}_i + \frac{\mathbf{I}}{\text{SNR}})^{-1}$ , then based on  $(\mathbf{P} + \epsilon^2 \mathbf{Q})^{-1} \approx \mathbf{P}^{-1} - \epsilon^2 \mathbf{P}^{-1} \mathbf{Q} \mathbf{P}^{-1}$  given small  $\epsilon^2$  we have the following,

$$\hat{\mathbf{W}}_i = (\mathbf{K}_i - \mathbf{K}_i (\mathbf{F}_i^* \mathbf{H}_i^* \Delta \mathbf{H}_i \mathbf{F}_i + \mathbf{F}_i^* \Delta \mathbf{H}_i^* \mathbf{H}_i \mathbf{F}_i) \mathbf{K}_i) \bullet (\mathbf{H}_i \mathbf{F}_i + \Delta \mathbf{H}_i \mathbf{F}_i)^*, \quad (13)$$

TABLE I: PHY layer simulation setup.

Communication system	IEEE 802.11ax
Link simulator	MATLAB WLAN Toolbox R2021b
Number of packets/simulation	20000
Channel type	IEEE TGax channel model-B [14]
Channel for each packet	i.i.d.
Speed of the scatter/user	0.089km/h
Channel coding	LDPC
Payload length	1000
MCS	5
Bandwidth	20 MHz (242 subcarriers in total)
Channel estimation error	ZMCSG
MIMO/MU-MIMO PHY	SVD/ZF precoding, MMSE decoding
CPU	Intel Core i7 CPU at 2.60GHz

where  $\Delta \mathbf{W}_i$  can be approximated as  $-\mathbf{K}_i (\mathbf{F}_i^* \mathbf{H}_i^* \Delta \mathbf{H}_i \mathbf{F}_i + \mathbf{F}_i^* \Delta \mathbf{H}_i^* \mathbf{H}_i \mathbf{F}_i) \mathbf{K}_i \mathbf{F}_i^* \mathbf{H}_i^* + \mathbf{K}_i \mathbf{F}_i^* \Delta \mathbf{H}_i^*$ .

$$\begin{aligned} &\mathbb{E}[(\hat{\mathbf{W}}_i \mathbf{H}_i \mathbf{F}_i) (\hat{\mathbf{W}}_i \mathbf{H}_i \mathbf{F}_i)^*] \\ &= \mathbb{E}[(\mathbf{W}_i + \Delta \mathbf{W}_i) \mathbf{H}_i \mathbf{F}_i] ((\mathbf{W}_i + \Delta \mathbf{W}_i) \mathbf{H}_i \mathbf{F}_i)^* \\ &= \mathbb{E}[\mathbf{W}_i \mathbf{H}_i \mathbf{F}_i \mathbf{F}_i^* \mathbf{H}_i^* \mathbf{W}_i^*] + \mathbb{E}[\Delta \mathbf{W}_i \mathbf{H}_i \mathbf{F}_i \mathbf{F}_i^* \mathbf{H}_i^* \Delta \mathbf{W}_i^*] \\ &= \mathbf{W}_i \mathbf{H}_i \mathbf{F}_i \mathbf{F}_i^* \mathbf{H}_i^* \mathbf{W}_i^* + \mathbf{E}_i \end{aligned} \quad (14)$$

where  $\mathbf{E}_i$  is obtained with property  $\mathbb{E}[\Delta \mathbf{H} \mathbf{A} \Delta \mathbf{H}] = \mathbb{E}[\Delta \mathbf{H}^* \mathbf{A} \Delta \mathbf{H}^*] = 0$  and  $\mathbb{E}[\Delta \mathbf{H} \mathbf{A} \Delta \mathbf{H}^*] = \sigma_e^2 \text{tr}(\mathbf{A}) \mathbf{I}$  in Eq. (9). The corresponding SINR is expressed as

$$\hat{\Gamma}_{i,j} = \frac{|(\mathbf{W}_i \mathbf{H}_i \mathbf{F}_i \mathbf{F}_i^* \mathbf{H}_i^* \mathbf{W}_i^* + \mathbf{E}_i)_{j,j}|^2}{\sum_{l \neq j} |(\mathbf{W}_i \mathbf{H}_i \mathbf{F}_i \mathbf{F}_i^* \mathbf{H}_i^* \mathbf{W}_i^* + \mathbf{E}_i)_{j,l}|^2 + [\mathbf{N}_i]_{j,j}}, \quad (15)$$

where

$$\begin{aligned} \mathbf{N}_i &= \mathbb{E}[\mathbf{W}_i \mathbf{n}_i \mathbf{n}_i^* \mathbf{W}_i^*] + \mathbb{E}[\mathbf{W}_i \mathbf{n}_i \mathbf{n}_i^* \Delta \mathbf{W}_i^*] + \mathbb{E}[\Delta \mathbf{W}_i \mathbf{n}_i \mathbf{n}_i^* \mathbf{W}_i^*] \\ &\quad + \mathbb{E}[\Delta \mathbf{W}_i \mathbf{n}_i \mathbf{n}_i^* \Delta \mathbf{W}_i^*] \end{aligned} \quad (16)$$

represents the expected noise power that can be further expressed in Eq. (10), using the property that  $\mathbb{E}[\Delta \mathbf{W}] = 0$ ,  $\mathbb{E}[\Delta \mathbf{H} \mathbf{A} \Delta \mathbf{H}] = \mathbb{E}[\Delta \mathbf{H}^* \mathbf{A} \Delta \mathbf{H}^*] = 0$  and  $\mathbb{E}[\Delta \mathbf{H} \mathbf{A} \Delta \mathbf{H}^*] = \sigma_e^2 \text{tr}(\mathbf{A}) \mathbf{I}$ . It is noteworthy that the channel matrix  $\mathbf{H}_i$  and  $\mathbf{F}_i$  in Eq. (15) are the ground truth matrices which are irrelevant to  $\sigma_e^2$ . This indicates that the MMSE detector  $\mathbf{W}_i$  in Eq. (15) is also the ground truth matrix as it follows Eq. (2). Afterwards, the analytical effective SINR under imperfect channel estimation is given by

$$\hat{\Gamma}_{eff}^{sindr} = -\hat{\beta} \ln \left( \frac{1}{n_{sc}} \frac{1}{n_s} \sum_{i \in \mathcal{N}_{sc}} \sum_{j=1}^{n_s} \exp \left( -\frac{\hat{\Gamma}_{i,j}}{\hat{\beta}} \right) \right), \quad (17)$$

where  $\hat{\Gamma}_{i,j}$  is expressed in Eq. (15), and  $\hat{\beta}$  is obtained from the simulation steps. Finally, the obtained effective SINR distribution under imperfect channel estimation is processed through the statistical steps, where the fitted log-SGN distribution follows  $\hat{X} \triangleq \ln(\hat{\Gamma}_{eff}^{sindr})$  expressed in Eq. (7).

## IV. VALIDATION

We validate effective SINRs following the simulation based flow chart through the ones from the analysis based flow

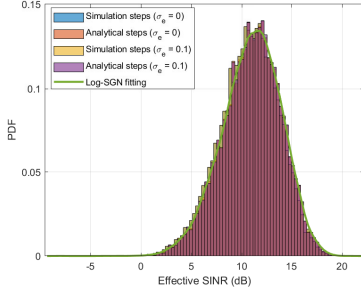


Fig. 6: Effective SINR distribution: Perfect/Imperfect channel estimation under  $2 \times 1$  MISO (SNR = 9dB) configuration.

chart under different OFDM scenarios. The main PHY layer simulation setup is summarized in Table I.

We first validate the MISO configuration shown in Fig. 6. The effective SINR distribution obtained from the analytical steps matches well with the one obtained from the simulation steps. Meanwhile, the effective SINR distributions overlap under perfect/imperfect channel estimation, which coincides with Lemma 1. Additionally, we use the log-SGN fitting method to get the log-SGN parameters characterized by Eq. (7). As the log-SGN fitting curve matches the analytical SINR distribution, the obtained log-SGN parameters accurately describe the system level performance under PHY layer configuration.

Moreover, we validate the developed methods under single-input and multiple-output (SIMO)/MIMO configuration. As Fig. 7 shows, the analytical effective SINR distribution fits with the corresponding the one obtained from the simulation steps under both configurations. Notice that compared with the SIMO configuration (Fig. 7(a) and (b)), the shapes of effective SINR distribution under MIMO configuration (Fig. 7(c) and (d)) are more divergent with the same setup of channel estimation quality. This is because the channel estimation error in under MIMO configuration impacts the post processing SINR more significantly than that under SIMO configuration. Similar to the MISO configuration, the log-SGN fitting curves also accurately characterizes the analytical effective SINR distributions under both configurations. Therefore, the log-SGN distribution can describe the effective SINR under all configurations considering the channel estimation error.

## V. CONCLUSION

In this letter, we investigated the EESM-log-SGN PHY layer abstraction with the channel estimation error. Two methods were developed to obtain the target PHY layer abstraction. The effective SINR was demonstrated to be irrelevant to the channel estimation error under MISO/SISO configuration. We validated that the effective SINRs from the analytical steps fitted with the ones from the simulation steps. Meanwhile, the log-SGN distribution is verified to accurately describe effective SINRs under imperfect channel estimation.

## REFERENCES

[1] S. Jin, S. Roy, and T. R. Henderson, "Efficient PHY layer abstraction for fast simulations in complex system environments," *IEEE Transactions on Communications*, vol. 69, no. 8, pp. 5649–5660, 2021.

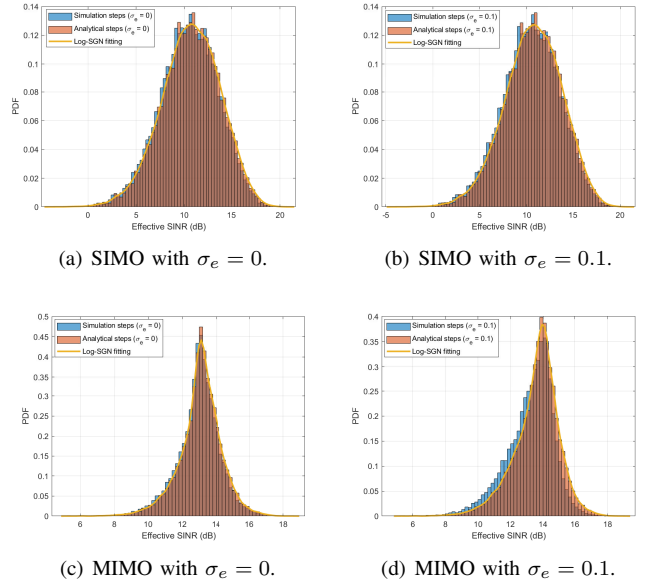


Fig. 7: Effective SINR distribution: Perfect/Imperfect channel estimation under  $1 \times 2$  SIMO (SNR = 9dB)/ $2 \times 2$  MIMO (SNR = 17dB) configuration.

[2] M. K. Müller *et al.*, "Flexible multi-node simulation of cellular mobile communications: the vienna 5G system level simulator," *EURASIP journal on wireless communications and networking*, vol. 2018, no. 1, pp. 1–17, 2018.

[3] R. P. F. Hoefel and O. Bejarano, "On application of PHY layer abstraction techniques for system level simulation and adaptive modulation in IEEE 802.11 ac/ax systems," *Journal of Communication and Information Systems*, vol. 31, no. 1, 2016.

[4] IEEE TGax Group, "IEEE p802.11 wireless lans: 11ax evaluation methodology," 2016.

[5] Mathworks, "Physical layer abstraction for system-level simulation," 2021.

[6] IEEE TGax Group, "Phy abstraction method comparison," in *IEEE 802.11-14/0647r2*, 2014.

[7] K. Brueninghaus *et al.*, "Link performance models for system level simulations of broadband radio access systems," in *2005 IEEE 16th International Symposium on Personal, Indoor and Mobile Radio Communications*, vol. 4. IEEE, 2005, pp. 2306–2311.

[8] L. Wan, S. Tsai, and M. Almgren, "A fading-insensitive performance metric for a unified link quality model," in *IEEE Wireless Communications and Networking Conference, 2006. WCNC 2006.*, vol. 4. IEEE, 2006, pp. 2110–2114.

[9] R. W. Heath Jr. and A. Lozano, *Foundations of MIMO Communication*. Cambridge University Press, 2018.

[10] Lei Wan, Shiauhe Tsai, and M. Almgren, "A fading-insensitive performance metric for a unified link quality model," in *IEEE WCNC*, vol. 4, 2006, pp. 2110–2114.

[11] A. H. Sayed, *Fundamentals of adaptive filtering*. John Wiley & Sons, 2003.

[12] E. Eraslan, B. Daneshrad, and C.-Y. Lou, "Performance indicator for MIMO MMSE receivers in the presence of channel estimation error," *IEEE Wireless Communications Letters*, vol. 2, no. 2, pp. 211–214, 2013.

[13] B. Hassibi and B. M. Hochwald, "How much training is needed in multiple-antenna wireless links?" *IEEE Transactions on Information Theory*, vol. 49, no. 4, pp. 951–963, 2003.

[14] IEEE TGax Group, "Ieee 802.11ax channel model document," 2014.

[15] Mathworks, "802.11ax packet error rate simulation for single-user format," 2021.

[16] —, "802.11ax packet error rate simulation for uplink trigger-based format," 2021.

[17] A. M. Cipriano, R. Visoz, and T. Salzer, "Calibration issues of PHY layer abstractions for wireless broadband systems," in *2008 IEEE 68th Vehicular Technology Conference*. IEEE, 2008, pp. 1–5.